# Seismological evidence for shallow thrusting north of the Timor trough

Robert McCaffrey, John Nábělek

*Geophys. J. R. astr. Soc.* (1986) **85,** 365–381

# Seismological evidence for shallow thrusting north of the Timor trough

Robert McCaffrey and John Nábělek *Department of Earth, Atmospheric and Planetary Sciences, Massachusetts Institute of Technology, Cambridge, MA 02139, USA*

Accepted 1985 September 30. Received 1985 August 2

**Summary**. The eastern Sunda arc in Indonesia is the site of subduction of the continental crust of Australia and its shallow seismicity is manifested by infrequent, large ($M_s \geq 7$) earthquakes that occur near the volcanic arc within the upper plate rather than as interplate events beneath the forearc. In the same region, volcanic activity has ceased and small shallow earthquakes are rare. We examine two of the larger earthquakes: the events of 1962 May 15 ($M_s = 7.2$) and 1977 August 27 ($M_s = 7.0$). The 1977 event occurred north of central Timor and the inversion of long-period *P*- and *SH*-waves indicates a nearly pure thrust mechanism at a depth of 10 km below sea-level and a seismic moment of $4.1 \times 10^{26}$ dyne cm. The *P*-wave nodal planes for this solution strike roughly parallel to the mapped trace of a thrust zone (the Wetar thrust zone) at the southern margin of the backarc basin and the south nodal dipping plane is consistent with the sense of thrusting on this thrust zone. A broad zone of compressional deformation is evident in seismic reflection profiles over the epicentral region of the 1977 event and gravity data suggest that a small amount of either isostatically uncompensated crustal thickening or flexure of the underthrusting plate has occurred. The 1962 earthquake occurred approximately 300 km north-east of the 1977 earthquake and near the eastern end of the volcanically quiet section of the Banda arc. The similarity of the few available waveforms to those at the same stations for the 1977 event suggests a similar source mechanism. Modelling of $P_{\text{dif}}$ waveforms for the 1962 event indicates a depth of less than 40 km and a preferred centroidal depth of 20 km, for which a seismic moment of $5 \times 10^{26}$ dyne cm is estimated. These fault plane solutions indicate that most of the seismic energy released by the collision between Australia and the Sunda arc is generated by faulting within the overriding plate and we infer that a major change in the plate geometry is imminent. We suggest that most of the relative convergence between the plates is accommodated by thrusting of the marginal

basin (the Banda Sea) southward beneath the arc and that the present geometry represents the initial stage of the reversal of the arc's polarity.

**Key words**: backarc thrusting, Indonesia

## 1 Introduction

The incipient collision between the Australian continent and the western Banda and eastern Sunda island arcs in eastern Indonesia provides a modern setting for studying arc–continent collision, a process thought to be of primary importance in the histories of several of the Earth's mountain belts. Several features that are anomalous compared to

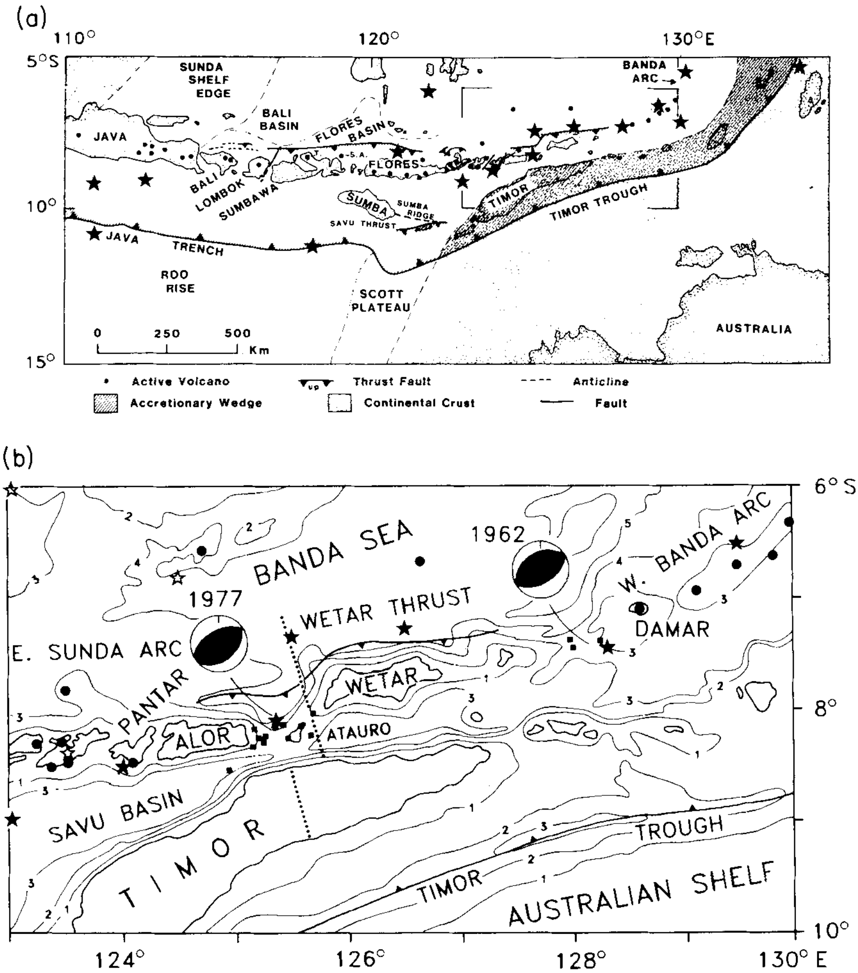


**Figure 1.** (a) Geographical and tectonic map of eastern Indonesia (from Silver *et al.* 1983). Stars show the positions of large ($M_S \geqslant 7$) earthquakes with focal depths of less than 100 km for the years 1897–1979. (b) Detail of region enclosed in brackets in (a). The locations of large earthquakes are shown by solid stars (depth $\leqslant 100$ km) and open stars (depth $> 100$ km). Bathymetry is adapted from Hamilton (1979) and Silver *et al.* (1983) and is contoured in kilometres. Lower hemisphere projections of the fault plane solutions for the 1962 and 1977 earthquakes are shown. Small squares mark the locations of aftershocks. The dotted line is the location of the gravity profile of Fig. 7.

areas where oceanic lithosphere is being subducted are evident along the eastern Sunda arc (Bowin *et al.* 1980; Hamilton 1979). The cause and effect relationships between the observed anomalies and the collision itself are uncertain, largely because few modern examples of arc–continent collision are available for comparison. In this paper we examine one of these anomalies – the tendency for large, shallow earthquakes to occur below the volcanic arc rather than beneath the forearc region as is normally the case in a subduction zone.

The earthquakes of 1962 May 15 and 1977 August 27 are two of 17 shallow (i.e. $h < 100$ km) events of $M_S \geq 7.0$ listed by Duda (1965) and Bath & Duda (1979) for the region along the Sunda arc between 110 and 135°E (Fig. 1). (We will refer to these $M_S \geq 7.0$ earthquakes as 'large' earthquakes.) Eight of these large earthquakes were located beneath the volcanic arc between 120 and 131°E, the section of the arc where continental crust is found beneath the Timor trough to the south. Along half of this section of the arc, from 124 to 129°E, volcanic activity has ceased. Shallow microearthquakes (McCaffrey *et al.* 1985) and intermediate sized earthquakes (Fig. 2), like volcanoes, are also nearly absent between 124 and 129°E. In the same region, the forearc is narrowest and the forearc ridge (Timor) comes in close proximity to the volcanic chain. Thus the correlation of the anomalies in volcanism and seismicity with the presence of the Australian continental margin in the subduction zone suggests a modification of the subduction process by the collision of the island arc with Australia.

In this paper we examine the two most recent of the large earthquakes from the arc region with the aim of understanding the mechanism of deformation of the arc by the collision. We infer that both earthquakes were thrust events in the upper 20 km of the overriding plate, indicating that a significant portion of the relative plate motion occurs along the boundary between the arc and the backarc basin.

## 2 Tectonic setting

Tectonic activity in south-east Indonesia is dominated by subduction of the Indian Ocean–Australian plate beneath the Sunda arc along the Java trench and Timor trough (Fig. 1a). From Java to Sumba, a region of subducting oceanic lithosphere, the subduction system is comparable in many ways to other oceanic subduction systems. The north-dipping slab of the Indian Ocean lithosphere, defined by earthquake hypocentres, extends from the trench

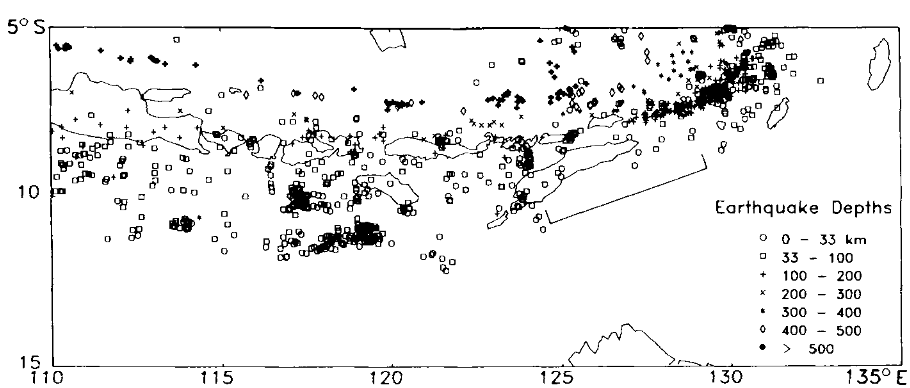


**Figure 2.** Epicentres of earthquakes along the eastern Sunda arc for the years 1964–79 recorded by 30 or more stations. The brackets outline the volcanically quiet zone between 124 and 129° E.

axis to over 600 km depth and its dip is nearly vertical from 300 to 600 km depth (Cardwell & Isacks 1978). McCaffrey *et al.* (1985) suggested that the concentration of earthquakes near 124°E beneath the eastern Savu Basin at 50–100 km depth originated at a tear in the Indian Ocean–Australian plate along the subducted continental–oceanic lithosphere boundary. The sense of motion along the tear inferred from fault plane solutions is consistent with oceanic lithosphere (to the NW) falling away from continental lithosphere (to the SE) along a NE-trending vertical fault within the subducted plate. The changes in volcanism and seismicity across the alleged tear may be due to a difference in the subduction angle caused by uneven buoyancy of the subducting plate and are similar to those observed in Chile and Argentina above tears in the descending Nazca plate (Barazangi & Isacks 1976; Jordan *et al.* 1983).

The Timor region of the arc, between 124 and 129°E, is anomalous in several respects and there are indications that some unknown amount of Australian continental crust has been subducted. Continental crust is found beneath the Timor trough (Curray *et al.* 1977; Jacobson *et al.* 1979) and various geological and geophysical observations suggest that it extends approximately 100 km arcward beneath Timor (Barber 1979; Bowin *et al.* 1980; Chamalaun, Lockwood & White 1976; Hamilton 1979; McCaffrey *et al.* 1985). The volcanic arc shows anomalous geochemical signatures east of Flores possibly owing to subduction of continental crust or shelf sediments (Morris 1983; Whitford *et al.* 1977). The volcanically quiet section from Pantar to Damar is approximately coincident with the narrowest and most elevated part of the forearc ridge (Timor) and deepest section of the Timor trough (SE of Timor). This section also appears to have fewer shallow earthquakes than the section of the arc to the west (Fig. 2) but in the past 90 years it has been the locus of several large ($M_S \geqslant 7$), shallow earthquakes located under the arc. The seismicity of the easternmost end of the arc is characterized by a slightly higher level of shallow activity than the Timor section and by a much larger number of intermediate and deep events than other sections of the arc.

A possible outcome of continent collision suggested by McKenzie (1969) is reversal of the polarity of the arc and subduction of the backarc basin. The present mode of deformation along the eastern Sunda arc supports the proposed scenario of McKenzie (Hamilton 1979; Silver *et al.* 1983). South directed thrusting behind the volcanic arc is observed from the Bali Basin to western Flores (Flores thrust zone) and from north of Alor to Romang (Wetar thrust zone) (Hamilton 1979, McCaffrey & Nábělek 1984a; Silver *et al.* 1983; Usna, Tjokrosapoetro & Wiryosujono 1979) and is associated with locally well developed accretionary prisms and negative gravity anomalies (Silver *et al.* 1983). The lateral extent of the

**Table 1.** Earthquake source parameters. Formal uncertainties are 1 standard deviation.

| Date | 1962 May 15 | 1977 August 27 |
|---|---|---|
| Origin time (hr: min: s) | 5:23:51 | 7:12:20 |
| Latitude (°S) | 7.44 | 8.10 |
| Longitude (°E) | 128.30 | 125.38 |
| Depth (km) ISC | 66 | 4 |
| Waveforms | 20 ± 5 | 10 ± 2 |
| Strike (°) | 54 ± 51 | 50 ± 2 |
| Dip (°) | 45 ± 3 | 39 ± 1 |
| Slip (°) | 90 ± 6 | 81 ± 1 |
| Moment ($10^{26}$ dyne cm) | 5.0 ± 0.2 | 4.11 ± 0.04 |
| Duration (s) | 10 | 13 |

Wetar thrust zone correlates well with the volcanically and seismically quiet zone north of Timor as discussed above. The Flores thrust zone, however, lies north of a volcanically and seismically active portion of the arc (Fig. 1) but, like the Wetar thrust zone, is associated with an elevated portion of the forearc (Sumba).

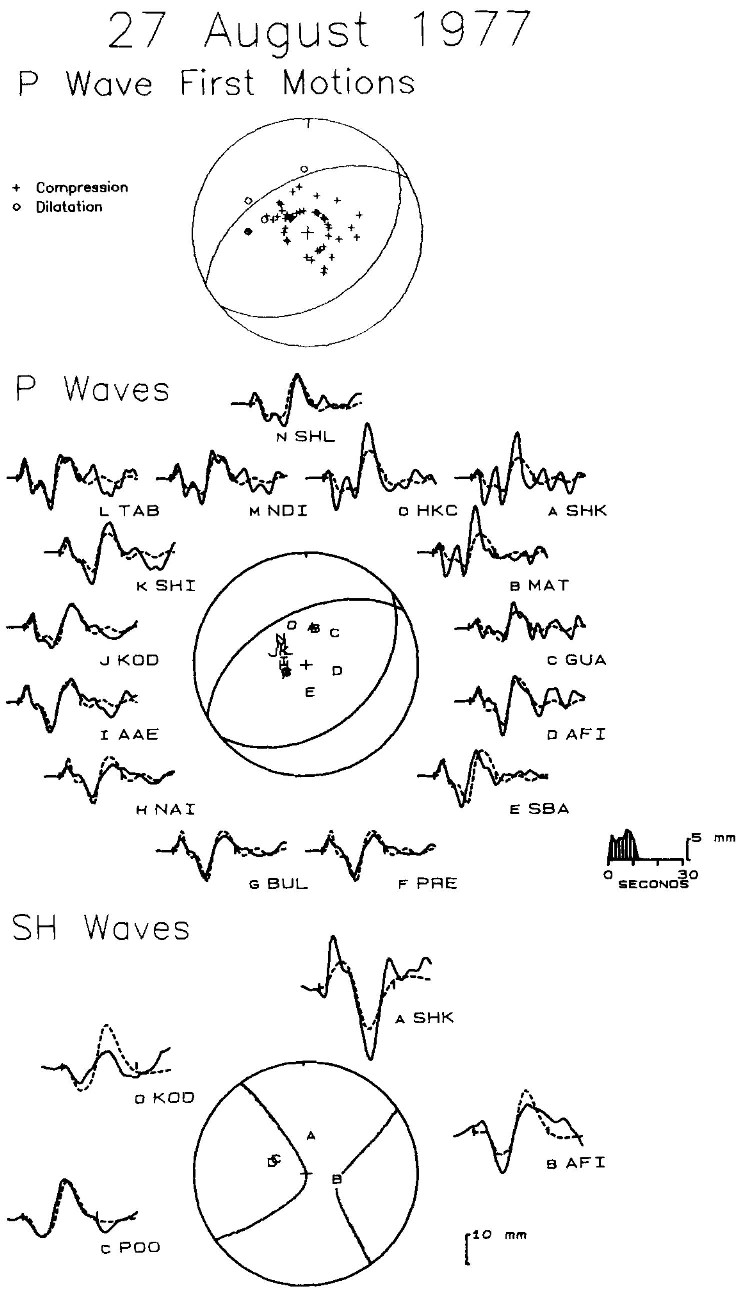


**Figure 3.** Fault plane solution for the 1977 earthquake. Calculated seismograms are shown with dotted lines and observed seismograms are the solid lines. Seismogram amplitudes are normalized to a common instrument magnification (300) and epicentral distance (40°). The estimated source time function is shown on the time-scale.

While there have been five major shallow earthquakes near the Wetar thrust zone in the past 90 years (Duda 1965; Bath & Duda 1979), the largest reported event on the Flores thrust zone is the magnitude 6.6 event in 1954 for which a poorly constrained mechanism has been determined (Wickens & Hodgson 1967). The largest well constrained thrust earthquakes to have occurred near the Flores thrust zone are the $m_b = 5.8$ event of 1978 at its eastern end (McCaffrey & Nábělek 1984a) and the $m_b = 6.1$ earthquake of 1979 that occurred beneath the Bali Basin at its western end (McCaffrey & Nábělek 1986). In the same region Duda (1965) listed a $M_s = 7.1$ earthquake in 1949 but at 80 km depth (Fig. 1).

## 3 The earthquake of 1977 August 27

The hypocentre of the 1977 earthquake determined by the International Seismological Centre (ISC) based on 419 $P$ arrivals (Table 1) is within the Wetar thrust zone north of Timor and about 20 km NW of Atauro Island (Fig. 1). Reports of two deaths and 25 injuries on Atauro (*Seismological Notes 1979*) suggest a shallow focus for the main shock. All shocks in the five weeks following the large earthquake (Fig. 1b) occurred to the south of the main event but the depths are poorly constrained. No foreshocks were reported by the ISC.

The fault plane solution (Fig. 3, Table 1) is constrained by the 15 $P$ and four $SH$ waveforms from long-period WWSSN instruments in the epicentral distance range of 30–95° and first motion polarities taken from regional and WWSSN short-period records. The source crustal structure used to generate the synthetic seismograms consisted of a water (ocean) layer over a homogeneous crust (Table 2). The main contribution to the seismograms comes

**Table 2.** Crustal structure used in calculation of seismograms.

| Depth to top of layer (km) | $v_p$ (km s$^{-1}$) | $v_s$ (km s$^{-1}$) | Density (g cm$^{-3}$) |
|---|---|---|---|
| Source | | | |
| 0 | 1.5 | 0.0 | 1.0 |
| 4* | 6.5 | 3.6 | 2.9 |
| Receiver | | | |
| Half-space | 6.0 | 3.4 | 2.7 |

* 3 km for 1962 earthquake.

from the direct waves ($P$ and $S$), the reflected phases from the water–crust interface ($pP$, $sP$ and $sS$), and the reverberations within the water. Values of $t^*$ of 1 s for $P$-waves and 4 s for $SH$-waves are used to account for anelastic attenuation. All waveforms, digitized at 0.5 s intervals, are inverted simultaneously for a point source orientation (double couple), depth, seismic moment, and source time function. The source time function is approximated by the trapezoid rule at 2 s increments. The inversion minimizes in a least squares sense the difference in observed and calculated seismogram amplitudes. The inversion procedure used here is described by McCaffrey (1986) and is similar to that of Nábělek (1984, 1985).

Observed and synthetic seismograms for the best fit solution are shown in Fig. 3 and the estimated parameters for the source centroid are given in Table 1. The fault plane solution shows high angle reverse faulting on either a NW- or SE-dipping plane with a small component of strike-slip. The largest contribution to the seismic moment comes from the first six elements of the source time function (Fig. 3); rupture duration was therefore approximately 12 s. The inclusion of a unilaterally propagating line source (Nábělek 1985) did not improve the fit, suggesting a bilateral rupture.

The source time function for this earthquake indicates that the moment release started slowly and increased abruptly after about 6 s. While this change in the time function is visible but not obvious in the long-period data, it is clear in the short-period seismograms (Fig. 4a). The large pulse in the short-period waveforms that occurs 6 s after the initial arrival must be due to the source time function rather than a depth phase because its amplitude is much too large to be due to a reflected phase (Fig. 4b). This observation is of interest because it shows that a sudden increase in the moment can cause confusion in the depth determination if prominent second arrivals picked from short-period records are assumed to be reflected phases. For example, the misidentification of this pulse as *pP* would lead to a depth estimate of 17 km for this earthquake.

In order to obtain a realistic estimate of the uncertainty in depth, the inversion of the long-period data was performed with the depth fixed at increments of 5 km (Fig. 5). The change in variance as a function of depth is shown in Fig. 6. The best fitting depth determined by the inversion of the long-period *P*- and *SH*-waves is 10 km. At this depth the source time function is the least complicated and is most consistent with the shapes of the short-period seismograms. From the formal uncertainty (Table 1), the width of the variance versus

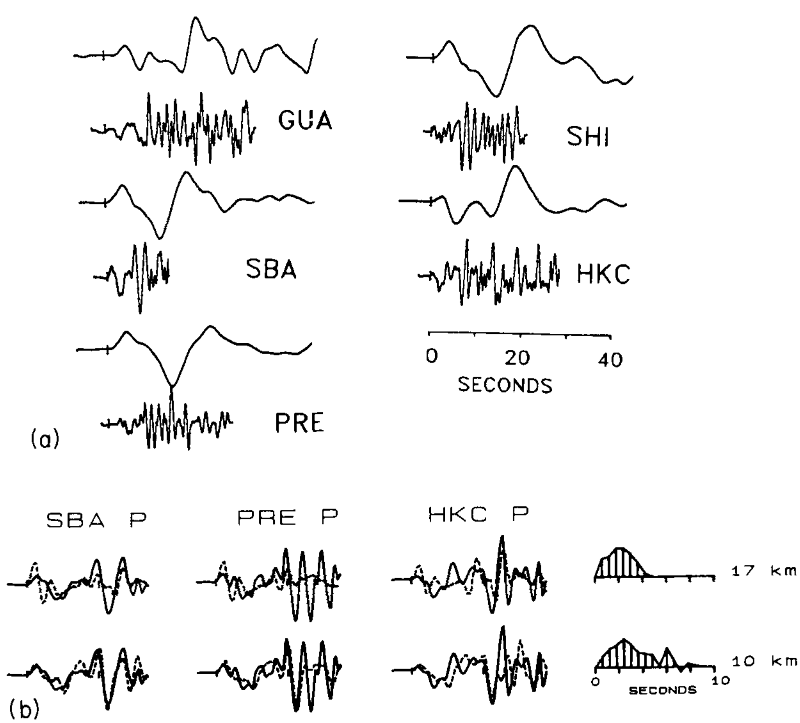


**Figure 4.** (a) Long-period (top) and short-period (bottom) waveforms for the 1977 earthquake plotted with the same time-scale. Note in the short-period data the consistency of the amplitude ratio between the initial phase (starting at the tic mark) and the sharp increase in energy that comes approximately 6 s later. (b) Synthetic short-period seismograms (dashed lines) calculated for the depths and source time functions shown and compared to the data (solid lines). In the top example we investigate the possibility that the late arriving, large amplitude arrivals are depth phases (*pP* or *sP*) by limiting the source time function to 5 s in length and inverting for its shape and the source depth. Note that the amplitude ratios between the initial and later arrivals are not matched. In the bottom example the source is shallow but the time function is lengthened and double peaked resulting in good agreement between the relative amplitudes. The short-period synthetics were generated with the same source structure and fault plane solution orientation as the long-period synthetics.

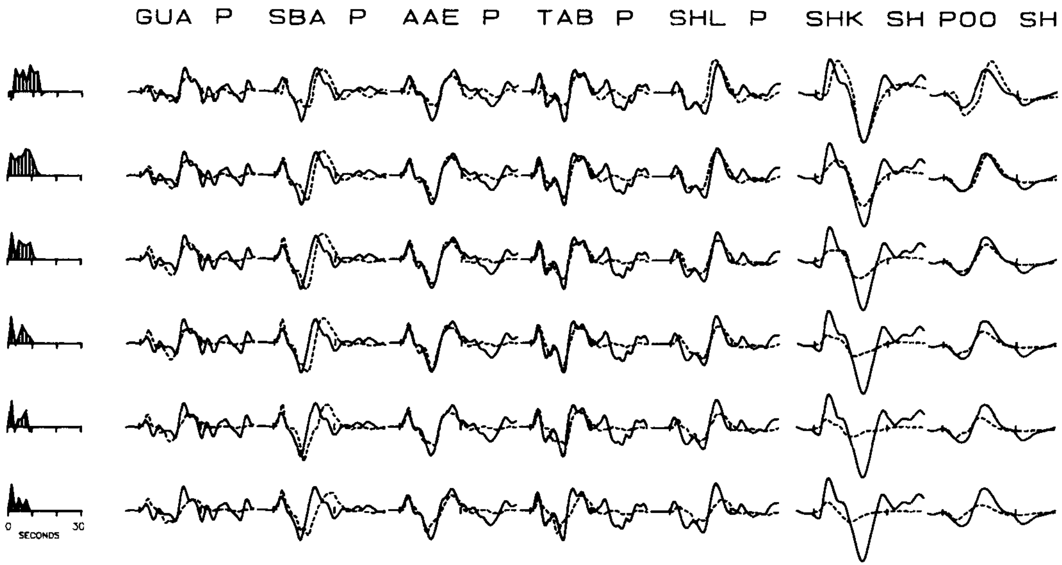


| Depth | Strike | Dip | Slip | Moment |
|---|---|---|---|---|
| 5 | 41 | 35 | 71 | 5.15 |
| 10 | 50 | 39 | 81 | 3.60 |
| 15 | 56 | 37 | 86 | 2.52 |
| 20 | 58 | 37 | 86 | 1.91 |
| 25 | 54 | 37 | 84 | 1.44 |
| 30 | 42 | 36 | 82 | 1.24 |

**Figure 5.** Waveform data for the 1977 earthquake compared with seismograms calculated at differing centroidal depths. Depth is in kilometres and moment is in $10^{26}$ dyne cm. The best fitting orientation and source time function were determined at each depth using all data. The solution at 10 km gives the best overall fit to the data and produces a source time function that agrees with the short-period data. Note also that the orientation varies little with the different assumed centroidal depths while the estimate of the moment is strongly dependent on the assumed depth.

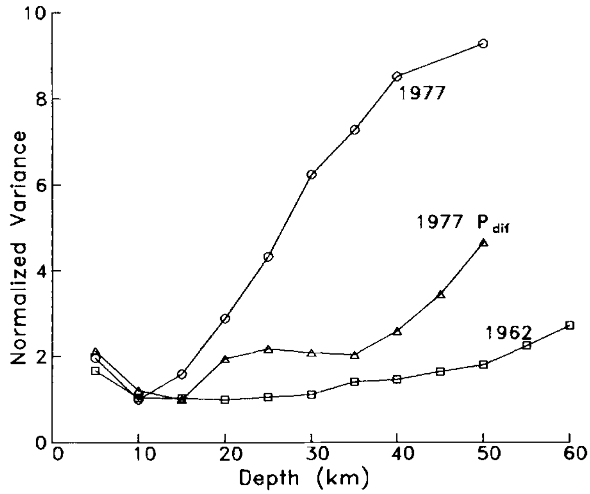


**Figure 6.** Calculated variance for the 1977 *P*-waves, 1977 $P_{\mathrm{dif}}$ waves, and 1962 $P_{\mathrm{dif}}$ waves as a function of source depth.

depth curve (Fig. 6) and by visual inspection of the waveforms in Fig. 5, we estimate an uncertainty in depth to be 5 km.

The long source time function (12 s) of the 1977 earthquake implies a large fault area. This, together with the centroidal depth (6 km below seafloor) and steep nodal planes, suggests that the earthquake ruptured the entire crust beneath the thrust zone.

## 4 Gravity over the Wetar thrust zone

Throughout its length the backarc thrust zone is associated with negative free-air gravity anomalies. The anomalies are in part due to thickening or downbowing of the crust by the thrusting and thus can be used to estimate the extent of the deformation. By making some assumptions about initial crustal thickness, we can also estimate the amount of crustal shortening needed to produce the increased thickness. From this estimate the rate or duration of thrusting can be inferred.

Along the Flores thrust zone the gravity anomalies reach below −100 mGal (Silver *et al.* 1983) and indicate either a strong deflection of the crust or considerable crustal thickening (McCaffrey & Nabelek 1984a). The gravity field over the Wetar thrust zone, however, shows a much smaller local minimum but nevertheless suggests that the crust is out of isostatic equilibrium. There has likely been some thickening or flexure of the Banda Sea crust beneath the thrust zone though much less than has occurred north of Flores.

In order to estimate the part of the gravity anomaly that is due to uncompensated crustal thickening, we compute the isostatic anomaly over the Wetar thrust zone. This is done by calculating the residual gravity for an isostatically balanced crustal model along the profile line shown in Fig. 1(b) (Fig. 7). In generating the cross-section we assume that at 50 km depth the total mass per unit area for a vertical column is $1.5 \times 10^7\,\mathrm{g\,cm^{-2}}$ using the densities shown. Sediments are ignored because their thickness is not known. Because sediments are deposited from above, they cannot be overcompensated by a crustal root and can contribute only positive isostatic anomalies. Therefore the isostatic anomalies we calculate may be biased in the positive sense, in which case our estimate of the uncompensated crustal thickening is a minimum. The structure we assume beneath the island of Timor is taken from

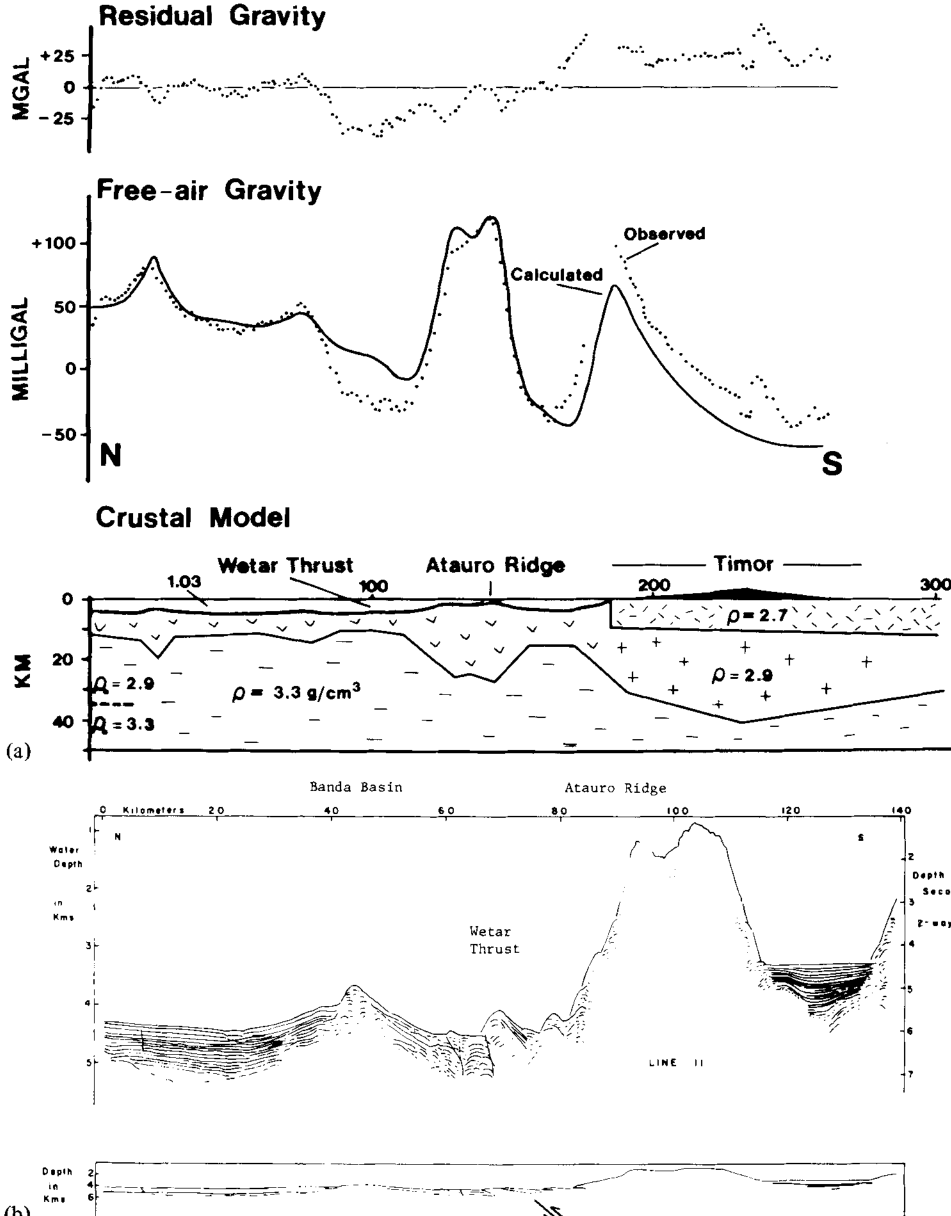


**Figure 7.** (a) Isostatically balanced crustal model and its gravity signature for the region of the Wetar thrust zone and Timor. Assumed densities for each layer are given in g cm$^{-3}$. Fig. 1(b) shows the location of this profile. Gravity data are taken from Chamalaun *et al.* (1976) and Silver *et al.* (1983). (b) Line drawing interpretation of a single channel seismic reflection profile over the Wetar thrust zone taken from Silver *et al.* (1983).

Chamalaun *et al.* (1976), but is required here to be in isostatic equilibrium. 30 mGal were added to the calculated gravity values in order to fit the observations over the north end of the profile. This shift is probably best explained by the contribution of the subducted slab (see McCaffrey & Nabelek 1984a). Relative to the isostatically balanced model, there is a low of 30 mGal over the Wetar thrust zone (Fig. 7).

A seismic reflection profile over the thrust zone (Fig. 7b) reveals a zone of south-dipping faults in the sedimentary layer above the source region of the 1977 earthquake. The small extent of the deformed zone indicates that only a small amount of convergence has occurred thus far. To estimate the amount of thickening from the gravity anomaly, we use the gravity calculation for an infinite sheet: $\delta g = 2\pi G\rho T$, where $\delta g$ is the gravity anomaly, $G$, is the gravitational constant, $T$ is the thickness of the sheet, and $\rho$ is its density or, in this case, the density contrast between the material that makes up the increased thickness of crust and the mantle it displaces. Assuming that thrusting within the crystalline crust produces the thickening, the $-30$ mGal isostatic anomaly over the Wetar thrust zone can be explained by an uncompensated increase in crustal thickness $T$ of about 1.8 km for a density contrast $\rho$ of $-0.4$ (2.9–3.3 g cm$^{-3}$) for the increased volume of crustal material. If the thickening proceeds by accreting sediments of density 2.3 g cm$^{-3}$ (i.e. $\rho = -1.0$ g cm$^{-3}$) rather than crust, then only a 0.7 km increase would be necessary to produce the observed gravity anomaly. These ranges of thickening within a 30 km wide basin of 6 km initial crustal thickness require 4–9 km of crustal shortening. In the case of flexure where water fills the void (i.e. $\rho = 2.3$ g cm$^{-3}$), the anomaly may be explained by a 0.3 km depression of the crust.

## 5 The earthquake of 1962 May 15

The epicentre of the 1962 earthquake is about 50 km SW of Damar Island (Fig. 1b), the westernmost active volcano of the Banda arc. No reports of damage have been found for this event. The earthquake occurred above an intermediate depth seismic zone characterized by intense activity at the bend in the Banda arc (Cardwell & Isacks 1978) and was originally assigned a depth of 66 km by the ISC.

We obtained nine $P$ waveforms for this event, none of which were in the epicentral distance range (30–90°) normally considered useful for waveform modelling. Seven were in the 100–127° range (i.e. $P_{\mathrm{dif}}$) and two were greater than 150° away (*PKP*) (Richter 1958). The waveforms are very similar to the ones from the 1977 earthquake recorded at the same

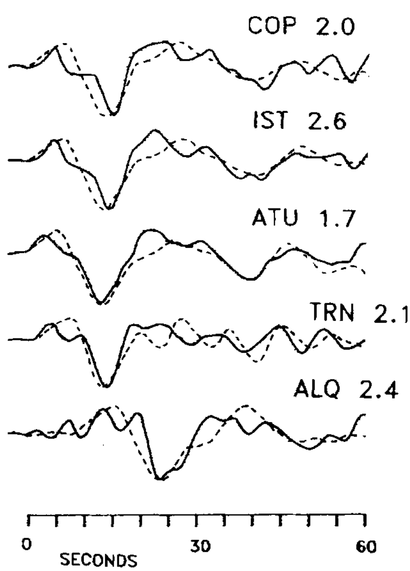


**Figure 8.** Comparison of the long-period waveforms from the 1962 (dashed lines) and 1977 (solid lines). The numbers following the station codes are the amplitude ratios between seismograms (1962 over 1977).

stations, suggesting that the 1962 earthquake had a similar mechanism (Fig. 8). The differences are essentially in the greater broadness and larger amplitudes of the seismograms for the 1962 event. Part of the broadness of the 1962 waveforms is due to the longer period response of the instruments used at the time but, as we show below, the broadness is primarily due to a longer time function and/or greater depth of the source.

We used the $P_{dif}$ waveforms from seven stations and 24 *P*-wave first motions to estimate the orientation, depth, and seismic moment of the 1962 earthquake (Table 3). All of the first motions that we examined were compressional (Fig. 9); therefore the inference of a predominantly thrust mechanism is strongly supported.

$P_{dif}$ travels as a compressional wave in the mantle and as a diffracted wave along the core–mantle boundary. Its take-off angles are essentially the same as for the *P*-wave at a delta of 100°. As with the *P*-wave, the $P_{dif}$ wave packet contains the direct *P* and reflected phases from structure above the source. The expected effect of the diffracted portion of the propagation path is to reduce the amplitudes drastically and to broaden the waveforms. In

**Table 3.** Data for seismograph stations used in the study.

| Station code | Phase | Delta (°) | Azimuth (°) | Take-off angle (°) |
|---|---|---|---|---|
| 1977 earthquake | | | | |
| SHK | *P* | 43.0 | 8.9 | 28.2 |
| SHK | *SH* | 43.0 | 8.9 | 28.2 |
| MAT | *P* | 46.0 | 14.4 | 27.4 |
| GUA | *P* | 29.0 | 42.2 | 31.4 |
| ALQ | $P_{dif}$ | 125.6 | 53.0 | 15.5 |
| TRN | *PKP* | 172.8 | 69.0 | – |
| AFI | *P* | 61.8 | 101.4 | 23.2 |
| AFI | *SH* | 61.8 | 101.4 | 23.2 |
| SBA | *P* | 72.9 | 171.6 | 20.3 |
| PRE | *P* | 92.9 | 243.6 | 15.7 |
| BUL | *P* | 93.5 | 249.2 | 15.6 |
| NAI | *P* | 88.4 | 268.9 | 16.1 |
| AAE | *P* | 87.9 | 279.4 | 16.2 |
| KOD | *P* | 51.0 | 290.1 | 26.0 |
| KOD | *SH* | 51.0 | 290.1 | 26.0 |
| POO | *SH* | 57.3 | 298.0 | 24.3 |
| SHI | *P* | 78.5 | 302.4 | 18.8 |
| ATU | $P_{dif}$ | 104.1 | 307.0 | 15.5 |
| TAB | *P* | 86.4 | 309.1 | 16.5 |
| IST | $P_{dif}$ | 100.0 | 310.0 | 15.5 |
| NDI | *P* | 59.1 | 310.3 | 23.8 |
| SHL | *P* | 46.7 | 316.8 | 27.2 |
| COP | $P_{dif}$ | 109.5 | 326.0 | 15.5 |
| HKC | *P* | 32.2 | 340.2 | 30.9 |
| 1966 earthquake | | | | |
| GOL | $P_{dif}$ | 122.3 | 47.4 | 15.5 |
| ALQ | $P_{dif}$ | 122.9 | 53.1 | 15.5 |
| TRN | *PKP* | 169.9 | 70.8 | – |
| ATU | $P_{dif}$ | 106.0 | 307.3 | 15.5 |
| IST | $P_{dif}$ | 101.9 | 310.3 | 15.5 |
| TOL | $P_{dif}$ | 126.6 | 314.9 | 15.5 |
| STU | $P_{dif}$ | 114.5 | 320.5 | 15.5 |
| COP | $P_{dif}$ | 10.6 | 327.0 | 15.5 |

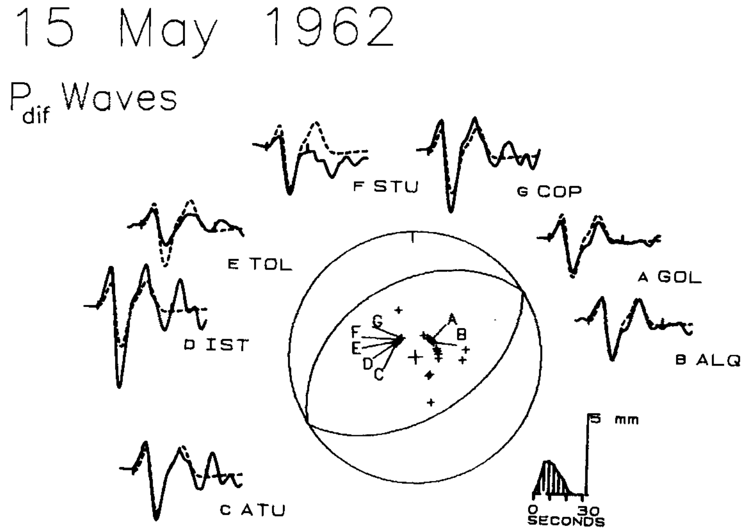


**Figure 9.** Fault plane solution and waveforms for the 1962 earthquake. The format is as in Fig. 3.

order to assess the feasibility of using $P_{\mathrm{dif}}$ seismograms, we examined the effect of using the $P_{\mathrm{dif}}$ seismograms from the 1977 event recorded at stations ALQ, ATU, IST, and COP on the determination of its depth, source time function, and moment. In the test, the orientation was fixed to the solution found from the closer stations and the best fitting source time function, moment and depth were determined. The preferred depth using the $P_{\mathrm{dif}}$ phases was 15 km, or only 5 km deeper than that determined with the seismograms from the closer stations but with a broad minimum in the variance (Fig. 6). At 10 km depth (the true centroidal depth), the moment was reduced by 30 per cent and the time function nearly doubled in length relative to the values found using the closer stations. These findings

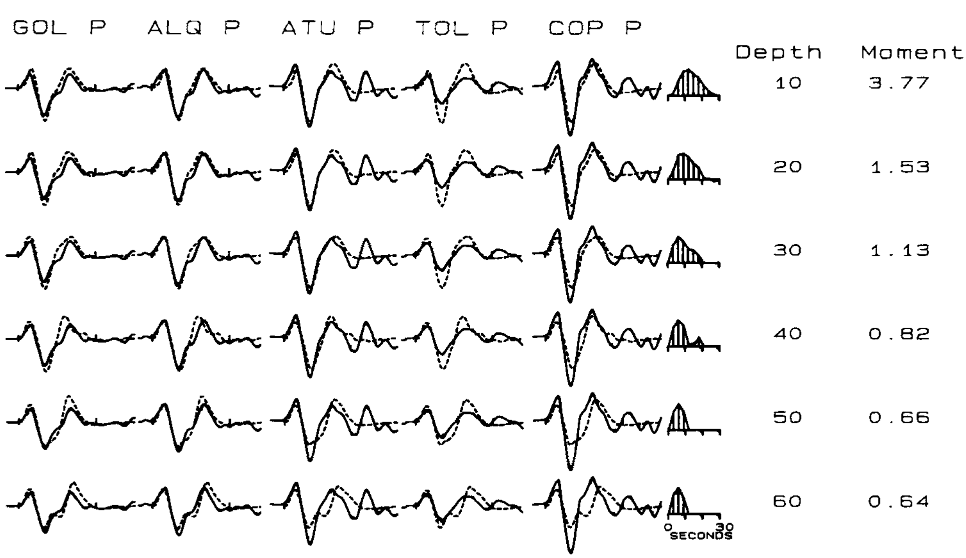


**Figure 10.** Results of inverting the $P_{\mathrm{dif}}$ waveforms of the 1962 earthquake for the source time function at 10 km depth intervals. Depth is in kilometres and moment is in $10^{26}$ dyne cm.

indicate that by using the $P_{dif}$ arrivals, the depth may be slightly overestimated, the moment is probably underestimated by about 30 per cent, and the source duration may be approximately two times too long.

The synthetics and source time functions computed for the 1962 event at several source depths are shown in Fig. 10 and the corresponding variances are shown in Fig. 6. The best fitting depth is at 20 km but the uncertainty is large (probably $\pm 20$ km or so) because of the broadness of the variance minimum (Fig. 6). From visual inspection, the waveforms in Fig. 10 indicate that the centroid is most likely above 40 km depth. Based on the bias estimates above, the corrected estimate of the seismic moment and duration for the source at 20 km depth are $5 \times 10^{26}$ dyne cm and 11 s, respectively.

The orientation of the mechanism shown in Fig. 9 produces the best fit to the seismograms but its strike is very weakly constrained. The estimated strike is likely because it is parallel to the arc in the epicentral region and is similar to that of the 1977 event.

## 6 Discussion

As was discussed briefly above, the eastern Sunda arc may be divided at 124°E on the basis of seismicity, volcanism, forearc morphology and the type of crust being subducted. The earthquakes described in this paper are the first shallow thrust faulting events to be found in the region east of 124°E and thus provide useful information on the direction of relative movements and type of deformation occurring within the collision zone between Australia and the eastern Sunda arc. West of 124°E and east of Java, along the Java trench, shallow seismicity is scattered throughout the forearc region (Fig. 2) and only one large event has been reported since 1890, namely the 1977 normal faulting event at 118°E (Fig. 1a). Elsewhere west of 124°E, published fault plane solutions for shallow earthquakes show a variety of thrust, normal, and strike-slip mechanisms (Cardwell & Isacks 1978; McCaffrey & Nábělek 1984b).

East of 124°E only two fault plane solutions for shallow events along the arc–trench system have been published previously and both show pure strike-slip with the compressional axes oriented roughly perpendicular to the local trend of the arc (Cardwell & Isacks 1978). The two events occurred near the bend in the arc; one in the backarc at 129°E and one in the forearc at 131°E. No fault plane solutions have been determined for events in the forearc region near Timor. Thus the 1962 and 1977 earthquakes are the only seismological evidence for crustal shortening within the region in which Australian continental crust has come in contact with the eastern Sunda and western Banda arcs.

Based on observations of vergence directions along the Wetar thrust zone from reflection profiles, evidence for Holocene uplift south of the thrust zone, and the form of bathymetric relief, we suggest that the south-dipping nodal plane represents the fault plane for the 1977 earthquake. Silver *et al.* (1983, fig. 7) show deformed sediments at the Wetar thrust zone bound in the north by a low angle, south-dipping fault. The position of the 1977 earthquake with respect to faults along the Wetar thrust zone (Fig. 7b) and the likelihood that it ruptured through to the seafloor suggest that it may have occurred on an extension of the surface faults into the basement. Reflection profiles across the Wetar thrust zone show that the majority of faults that appear to cut the entire sedimentary section dip to the south (Silver *et al.* 1983). South of the thrust zone, Atauro and parts of Timor show marine terraces at several hundred metres elevation and have had an average uplift rate of 0.5 mm $yr^{-1}$ over the past 120 000 years (Chappell & Veeh 1978). Finally, because the volcanic chain stands approximately 5 km higher and is less dense than the oceanic crust to the north, it is likely that it will form the overriding plate when thrusting occurs.

If large, shallow earthquakes are the predominant means of producing crustal shortening (at least over the past 90 years), then the distribution of large earthquakes along the eastern Sunda arc indicates that most recent convergence within the collision zone has been taken up in the backarc region. Hamilton (1979), however, showed several reflection profiles over the Timor trough south of Timor (his figs 73 and 74) that indicate bending of the Australian continental shelf into the trench and deformation of the trench sediments. Thus the eastern Sunda arc represents a two sided block bound by thrust faults with opposite vergence directions (Fig. 11) and with very different responses to the collision process. While the

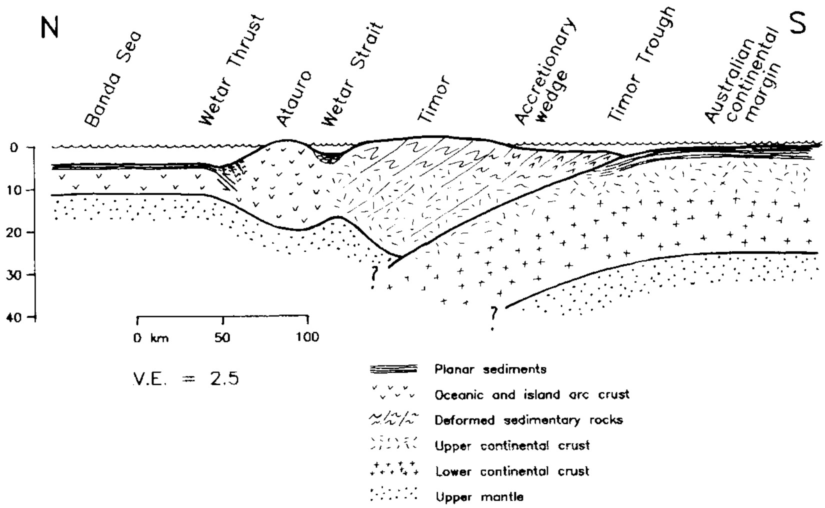


**Figure 11.** Schematic NW–SE cross-section of the eastern Sunda arc near Timor. The opposing arrows beneath the Wetar thrust zone show the position of the 1977 earthquake.

backarc thrust zone is seismically energetic, underthrusting at the Timor trough must proceed aseismically or by the occurrence of infrequent large events. The difference in reactions to the collision may be related to the type of crust involved, the stage of development of the thrust zones themselves, or both. Possibly the weak continental crust in the well developed thrust zone to the south creeps or fractures with little stress drop while the stronger, newly fractured oceanic crust north of the volcanic arc builds up large stresses before breaking.

The Wetar thrust zone appears to be poorly developed in comparison with the Flores thrust zone to the west even though it is situated across the arc from where the Australian continent impinges most directly on the Timor trough (Fig. 1a). The Flores thrust zone displays a broader and more extensively deformed accretionary prism as well as more negative gravity anomalies than does the Wetar thrust zone (Silver *et al.* 1983; McCaffrey & Nábělek 1984a). The advanced stage of the Flores thrust zone is likely to be due to a longer history or faster rate of underthrusting there. The Flores thrust zone, like the Timor trough, is much quieter seismically than the Wetar thrust zone except at its ends where it is probably encroaching on new crust (Fig. 1a; McCaffrey & Nábělek 1984a, b).

The strong contrast in the developmental stages of the Wetar and Flores thrust zones suggests that their causes are not the same. While the Wetar thrust zone is developing in response to the late Pliocene collision of the arc with Australia, the development of the Flores thrust zone is probably tied to the interaction of the arc with the Sumba Ridge, a piece of thickened crust (containing Sumba Island) trapped in the forearc during the Early

Miocene initiation of the Java trench (Otofuji *et al.* 1981; Reed *et al.* 1986). The presence of Sumba is also tied to shallow interplate, underthrusting earthquakes which in the forearc east of Java are found only beneath the Sumba Ridge and at a depth close to the crustal thickness of the ridge (McCaffrey & Nábělek 1984b). Thus the Sumba Ridge represents an anomaly in the distribution of stress within the forearc and it may act to transmit compressive stresses from the downgoing plate to the arc.

High angle thrust earthquakes behind volcanic arcs are observed in other areas of the world, notably east of the Andes (Suarez, Molnar & Burchfiel 1983; Jordan *et al.* 1983), west of Japan (Boyd, Mori & Suarez 1984; Yoshii 1979), along the Muertos trough (Byrne, Suarez & McCann 1984), and west of the Sangihe arc in the northern Molucca Sea (Stewart & Cohn 1979). Of these, only the last example involves a collision that is producing a major realignment of plate geometry rather than merely a fragmentation of the overriding plate. The present interaction between Australia and the eastern Sunda arc is described best as a collision event because subduction in the forearc has been significantly modified and a jump in the locus of relative plate motion to the Wetar thrust zone is underway. Major geological consequences of the shift in the site of convergence to the backarc region are the accretion of the volcanic islands and Timor to the Australian plate and building of a new trench–island arc structure of the opposite polarity on top of the old.

## Acknowledgments

We thank E. A. Silver and B. L. Isacks for critical reviews. This work was supported by National Science Foundation Grants EAR-8115909 and EAR-8319250 and United States Geological Survey Grant 14-08-0001-G-959.

## References

Barazangi, M. & Isacks, B. L., 1976. Spatial distribution of earthquakes and subduction of the Nazca plate beneath South America, *Geology*, **4**, 686–692.

Barber, A. J., 1979. Structural interpretations of the island of Timor, eastern Indonesia, in *Proc. S.E. Asian Petrol. Expl. Soc.*, **IV**, 9–21.

Bath, M. & Duda, S. J., 1979. Some aspects of global seismicity, *Tectonophys.*, **54**, T1–T8.

Bowin, C. O., Purdy, G. M., Johnston, C., Shor, G. G., Lawver, L., Hartono, H. M. S. & Jezek, P., 1980. Arc-continent collision in the Banda Sea region, *Bull. Am. Ass. Petrol. Geol.*, **64**, 868–915.

Boyd, T., Mori, J. & Suarez, G., 1984. Fault plane determination of the 1964 Niigata, Japan earthquake (abstract), *Eos, Trans. Am. geophys. Un.*, **65**, 1016.

Byrne, D. E., Suarez, G. & McCann, W. R., 1984. Seismological evidence for subduction of the Caribbean plate beneath Hispaniola along the Muertos trough (abstract). *Eos, Trans. Am. geophys. Un.*, **65**, 1108.

Cardwell, R. K. & Isacks, B. L., 1978. Geometry of the subducted lithosphere beneath the Banda Sea in eastern Indonesia from seismicity and fault plane solutions, *J. geophys. Res.*, **87**, 2825–2838.

Chamalaun, F. H., Lockwood, K. & White, A., 1976. The Bouguer gravity field of eastern Timor, *Tectonophys.*, **30**, 241–259.

Chappell, J. & Veeh, H. H., 1978. Late Quaternary tectonic movements and sea-level changes at Timor and Atauro island, *Bull. geol. Soc. Am.*, **89**, 1189–1198.

Curray, J. R., Shor, G. G., Raitt, R. W. & Henry, M., 1977. Seismic refraction and reflection studies of crustal structure of the eastern Sunda and western Banda arcs, *J. geophys. Res.*, **82**, 2479–2489.

Duda, S. J., 1965. Secular seismic energy release in the circum-Pacific belt, *Tectonophys.*, **2**, 409–452.

Hamilton, W., 1979. Tectonics of the Indonesian region, *Prof. Pap. U.S. geol. Surv. 1078.*

Jacobson, R. S., Shor, G. G., Kieckhefer, R. M. & Purdy, G. M., 1979. Seismic refraction and reflection studies in the Timor-Aru trough system and Australian continental shelf, *Mem. Am. Ass. Petrol. Geol.*, *29*, 209.

Jordan, T. E., Isacks, B. L., Allmendinger, R. W., Brewer, J. A., Ramos, V. A. & Ando, C. J., 1983. Andean tectonics related to geometry of subducted Nazca plate, *Bull. geol. Soc. Am.*, **94**, 341–361.

McCaffrey, R., 1986. Focal depths and mechanism of the larger earthquakes along the eastern Sunda arc from waveform analyses, *J. geophys. Res.*, submitted.

McCaffrey, R., Molnar, P., Roecker, S. & Joyodiwiryo, Y., 1985. Micro-earthquake seismicity and fault plane solutions related to arc-continent collision in the eastern Sunda arc, Indonesia, *J. geophys. Res.*, **90**, 4511–4528.

McCaffrey, R. & Nábělek, J., 1984a. The geometry of backarc thrusting along the eastern Sunda arc, Indonesia: constraints from earthquake and gravity data, *J. geophys. Res.*, **89**, 6171–6179.

McCaffrey, R. & Nábělek, J., 1984b. Depths and source mechanisms of earthquakes from the eastern Sunda arc, Indonesia (abstract), *Eos, Trans. Am. geophys. Un.*, **65**, 997.

McCaffrey, R. & Nábělek, J., 1986. Earthquakes, gravity, and the origin of the Bali Basin, *J. geophys. Res.*, submitted.

McKenzie, D. P., 1969. Speculations on the consequences and causes of plate motion, *Geophys. J. R. astr. Soc.*, **18**, 1–18.

Morris, J. D., 1983. Continental contamination in the Banda arc: Pb-Nd isotopic evidence for 3-component mixing, *Eos, Trans. Am. geophys. Un.*, **64**, 906.

Nábělek, J., 1984. Determination of earthquake source parameters from inversion of body waves, *PhD thesis*, Massachusetts Institute of Technology.

Nábělek, J., 1985. Geometry and mechanism of faulting of the 1980 El Asnam, Algeria, earthquake from inversion of teleseismic body waves and comparison with field observations, *J. geophys. Res.*, **91**, 12 713–12 728.

Otofuji, Y., Sassajima, S., Nishimura, S., Yokoyama, T., Hadiwisatra, S. & Hehuwat, F., 1981. Paleomagnetic evidence for the paleoposition of Sumba island, Indonesia, *Earth planet. Sci. Lett.*, **52**, 93–100.

Reed, D. L., Silver, E. A., Prasetyo, H. & Meyer, A. W., 1986. Time-transgressive overlap assemblage and erosion on a Quaternary terrane suture, eastern Sunda forearc, Indonesia, *Geology*, submitted.

Richter, C. F., 1958. *Elementary Seismology*, W. H. Freeman, San Francisco.

Seismological Notes, 1979. *Bull. seism. Soc. Am.*, **69**, 653.

Silver, E. A., Reed, D. R., McCaffrey, R. & Joyodiwiryo, Y. S., 1983. Backarc thrusting in the eastern Sunda arc, Indonesia: a consequence of arc-continent collision, *J. geophys. Res.*, **88**, 7448.

Stewart, G. S. & Cohn, S. N., 1979. The 1976 August 16, Mindanao, Philippine earthquake – evidence for a subduction zone south of Mindanao, *Geophys. J. R. astr. Soc.*, **57**, 51–65.

Suarez, G., Molnar, P. & Burchfiel, C., 1983. Seismicity, fault plane solutions, depth of faulting, and active tectonics of the Andes of Peru, Ecuador, and southern Colombia, *J. geophys. Res.*, **88**, 10 403–10 428.

Usna, I., Tjokrosapoetro, S. & Wiryosujono, S., 1979. Geological interpretation of a seismic reflection profile across the Banda Sea between Wetar and Buru islands, *Bull. Geol. R. Dev. Centre*, **1**, 7–15.

Whitford, D. J., Compston, W., Nicholls, I. A. & Abbott, M. J., 1977. Geochemistry of late Cenozoic lavas from eastern Indonesia: role of subducted sediments in petrogenesis, *Geology*, **5**, 571–575.

Wickens, A. J. & Hodgson, J. H., 1967. Computer re-evaluation of earthquake mechanism solutions 1922–1962, *Publ. Dom. Obs., Ottawa*, **33**.

Yoshii, T., 1979. A detailed cross-section of the deep seismic zone beneath northeastern Honshu, Japan, *Tectonophys.*, **55**, 349–360.